IEEE Access
Multidisciplinary | Rapid Review | Open Access Journal

Received 27 May 2024, accepted 3 June 2024, date of publication 7 June 2024, date of current version 18 June 2024.

Digital Object Identifier 10.1109/ACCESS.2024.3411393

RESEARCH ARTICLE

Ridge Gap Waveguide Low Pass Filters: A Systematic Design Approach

MAHMOUD GADELRAB[1], (Student Member, IEEE), SHOUKRY I. SHAMS[1], (Senior Member, IEEE), MAHMOUD ELSAADANY[2], (Senior Member, IEEE), AND ABDELRAZIK SEBAK[1], (Life Fellow, IEEE)

[1]Electrical and Computer Engineering Department, Concordia University, Montreal, QC H3G 1M8, Canada
[2]Computer Science Department, MacEwan University, Edmonton, AB T5J 4S2, Canada

Corresponding author: Mahmoud Gadelrab (Mahmoud.gadelrab@ieee.org)

ABSTRACT In satellite communication systems, Low Pass Filters (LPFs) are used to remove harmonics generated from the power source, minimize interference, and enhance the signal-to-noise ratio. Through the filter design process, various aspects must be considered such as the insertion loss, bandwidth, weight, and size. A stepped Impedance filter is a typical topology to realize the LPFs. The stepped impedance filter design process goes through multiple design steps starting from the normalized prototype design and ending with the realization of the filter sections. The filter realization significantly depends on the host guiding structure. This paper, presents, for the first time, a systematic design approach for the stepped impedance filter based on ridge gap waveguide technology. An accurate mathematical model for calculating a virtual cutoff for the ridge gap waveguide is introduced, which is deployed in the proposed design methodology. Moreover, a prototype of the stepped impedance filter is fabricated and measured, with measured results closely aligning with simulations.

INDEX TERMS Low pass filter (LPF), ridge gap waveguide (RGW), stepped impedance filter, transverse resonance method.

I. INTRODUCTION

Communication systems have evolved significantly since the deployment of the initial Intelsat satellite series in the late 1960s. Over the past four decades, satellite systems have broadened their scope from conventional fixed telecommunication to encompass mobile, navigation, and remote-sensing applications [1], [2]. These satellites' payloads include critical microwave components like orthomode transducers, couplers, antennas, and filters. Filters, depending on the service objectives and applications, span various frequency ranges. Navigation and mobile satellite systems primarily operate in the L (1-2 GHz) and S-band (2-4 GHz), while remote sensing applications predominantly utilize the C-band (4-8 GHz). In video/audio transmission, the growing demand for high-quality services has led to the expansion of the frequency band towards the Ku-band (12-18 GHz), with exploration into higher spectral bands (20-30 GHz) [3], [4], [5].

Many different applications, including satellite communications and ground stations, frequently employ stepped impedance filters [6], [7], [8]. The frequency specification of the low-pass filter must meet a variety of requirements depending on the application. The filter's major aspects are the pass-band frequency range, the high rejection level, and the deep in-band matching level. These challenging requirements need significant effort to develop a variety of innovative solutions providing different compromises. Rectangular waveguide filters are considered among the highly visited low-pass configurations due to the matching level, the low loss, and the simplicity of construction. However, the realization challenges become significant at high-frequency bands due to the difficulty of ensuring proper electrical contact between the fabricated parts [9].

The associate editor coordinating the review of this manuscript and approving it for publication was Photos Vryonides.

RGW is a promising mm-wave technology first introduced in 2009 [10] as a TEM guiding structure that results in minimal dispersion. It is based on the concept of hard and soft surfaces [11], which provides numerous benefits such as self-packaging and a wide range of bandwidth. Moreover, it exhibits excellent electrical characteristics in terms of losses at higher frequencies as the signal is propagating inside an air gap [12]. The operational bandwidth of the gap waveguide relies on the stop band of the cell structure featuring an artificial magnetic conductor surface. Consequently, optimizing unit cells to achieve the broadest stop band becomes essential. Diverse unit cell designs have been explored, resulting in bandwidth ratios around 2:1 in some studies, while others have achieved ratios surpassing 3:1 [13], [14], [15]. Whether employed to contain ridge leakage or package transmission lines, the bandwidth of these periodic cells serves as a pivotal metric to evaluate their performance. The evolving landscape of RGW unit cells underscores their critical role in the realization of efficient waveguide systems.

This technology has been tested and validated in numerous publications, such as hybrid couplers, magic tee, phase shifter, circulators, and antennas [17], [18], [19], [20], [21]. However, few published articles proposed filter design in general and low-pass filters specifically. Recently, various band-pass filter designs have been presented and validated through measurements [22], [23], [24]. The hosting guides for most of these articles are groove gap waveguide [24] or Inverted-Microstrip Ridge Gap [25], [26]. This technology is used to provide diplexers as well as filters in high-frequency bands [27], [28]. All the previously published filter designs addressed the design of bandpass filters through multiple cavities, whereas no single design addressed the design procedure needed for low-pass filters based on the stepped impedance technique.

In this article, we propose, for the first time, a systematic design approach for low-pass filters based on RGW. We present an approximate mathematical equation to calculate the propagation constant inside the ridge gap waveguide. This equation is derived through the transverse resonance method, accounting for ridge and bed of nail discontinuities. The proposed mathematical model provides initial parameters for designing an RGW low-pass filter. To validate this equation, two filters were designed for different bands, namely the X and Ka bands. The X-band filter is fabricated and measured using a ridge waveguide transition showing a good matching level of about -16.8 dB. Moreover, the insertion loss is in the range of 0.7 dB, and the rejection is below 40 dB.

The paper is organized as follows: Section II presents the proposed mathematical model to obtain the propagation constant. In Section III, we present the design procedure. Afterward, the fabricated prototype is illustrated along with the comparison between the simulated and the measured results. Section IV criticizes and compares the proposed design with other RGW filter designs in the literature.

TABLE 1. Unit cells dimensions.

X-band	Value (mm)	Ka-band	Value (mm)
a_{pin}	**6.5**	a_{pin2}	**1.96**
b	**3.2**	b_2	**2.32**
gap	**0.2**	gap_2	**0.36**
Wpin	**3**	$Wpin_2$	**0.78**
Hpin	**3**	$Hpin_2$	**1.96**

Finally, the contributions are summarized in the conclusion section.

II. MATHEMATICAL MODEL OF THE RGW FILTER SECTIONS

The proposed filter design is based mainly on the idea of a stepped impedance filter, where sections of high and low characteristic impedance are alternately used [29]. This is approximated in a circuit utilizing alternating capacitive and inductive impedances. A stepped ridge structure can perform the same concept, where small gaps and large gaps represent high impedance (inductive) and low impedance (capacitive) respectively. Therefore, it is required to calculate the ridge width and gap. In the next subsection, we are going to define the shape and dimensions of the unit cell used in this RGW structure. Afterward, a mathematical model is proposed to give accurate initial values for the ridge dimensions and the gaps.

A. UNIT CELL

The main objective for the RGW is to create a parallel plate stop band using a periodic structure. The cell dimensions selection is controlled by the filter operating bandwidth as well as the rejection band. This will be explained in a later section, where the filter specifications will be addressed.

1) X-BAND

The unit cell used here is a cube-shaped pin ($H_{pin} = W_{pin}$) with dimensions shown in Table 1. The dispersion diagram for the unit cell of this periodic structure is shown in Figure 1 (a). This diagram is calculated using the Eigenmode Solve in CST Microwave Studio where it shows that the pass band is from 10 GHz to 30GHz.

2) KA-BAND

The other unit cell is in the shape of a cuboid where ($H_{pin2} \neq W_{pin2}$) and the dimensions are in Table 1, and its passband is from 30 to 60 GHz.

B. PROPAGATION CONSTANT CALCULATION

In designing the equiripple low pass filter, the propagation constant β should be determined. Afterward, the number of steps should be determined based on the required rejection. In addition, the required level of the ripple will guide the normalized prototype used in the design. Finally, the electrical length of the inductors and capacitors sections are

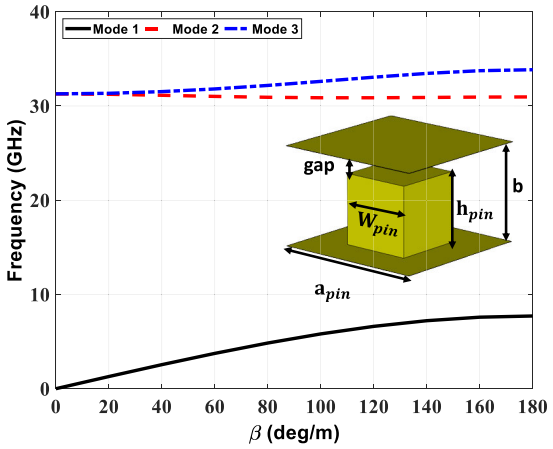

FIGURE 1. Dispersion diagram for the X-band unit cell.

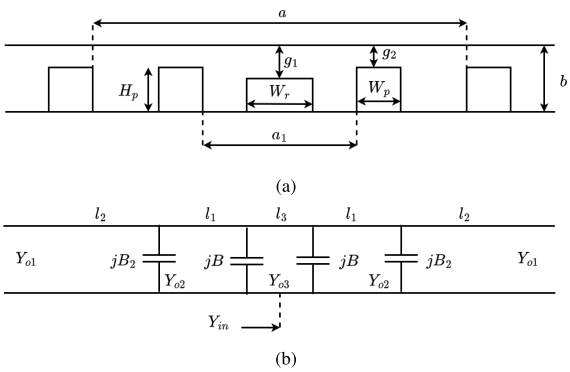

FIGURE 2. Equivalent model, (a) Schematic and (b) Transmission Line.

determined using the following equations [29],

$$\beta l = \frac{LZ_o}{Z_h} \tag{1}$$

$$\beta l = \frac{CZ_l}{Z_o} \tag{2}$$

such that Z_o is the filter impedance, L and C are the normalized element values of the low-pass prototype that can be obtained from the normalized design tables. In order to implement such a filter in RGW waveguide technology we need to determine the ridge width, ridge gap, capacitive and inductive gaps, and lengths. An efficient model is proposed, where good initial values for the aforementioned parameters are calculated. In our model, we calculate a virtual cutoff propagation constant k_c using the transverse resonance method such that the side walls here are assumed to be a perfect open circuit.

It is worth mentioning that the RGW dominant mode is quasi-TEM mode. Accordingly, assuming the propagation constant is exactly equal to the free space wave number leads to a poor filter design. The proposed novel methodology can provide a more accurate evaluation of the phase constant value, which leads to a better filter initial design. The effect of the first pin is taken into consideration as a capacitive

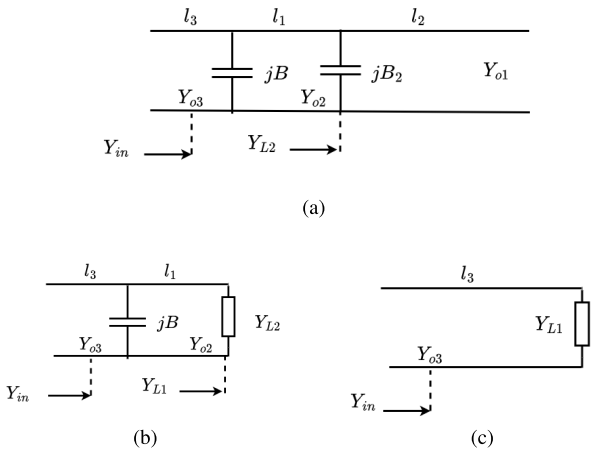

FIGURE 3. Load admittance calculations, (a) Section II, (b) Section I, and (c) Input admittance.

discontinuity. The physical variables defining the RGW are separately indicated in the diagram 2 (a). When applying the transverse resonance method, operation at cutoff is assumed, and the fields have no z dependence. An excellent approximation to represent the RGW as six parallel-plate waveguides along the X direction with spaces g_1, g_2, and b. Therefore, it can be analyzed as six transmission lines, as in Figure2 (b). The lengths of the transmission lines are,

$$l_1 = (a_1 - W_r)/2 \tag{3}$$

$$l_2 = (a - a_1 - W_p)/4 \tag{4}$$

$$l_3 = W_r/2 \tag{5}$$

where the length of the second transmission line is assumed to be half the way between the two pins. This approximation is valid in the proposed model as the open circuit is assumed to be perfect at this point. Moreover, the characteristic impedance of each transmission line can be expressed as follows,

$$Y_{o1} = \frac{k_c}{\omega\mu}(\frac{1}{b}) \tag{6}$$

$$Y_{o2} = \frac{k_c}{\omega\mu}(\frac{1}{g_2}) \tag{7}$$

$$Y_{o3} = \frac{k_c}{\omega\mu}(\frac{1}{g_1}) \tag{8}$$

and the capacitive discontinuities are calculated as [31],

$$\frac{B}{Y_{o1}} = \frac{8\pi b}{k_c} ln(\csc\frac{\pi g_1}{2b}) \tag{9}$$

$$\frac{B_2}{Y_{o2}} = \frac{8\pi b}{k_c} ln(\csc\frac{\pi g_2}{2b}) \tag{10}$$

At the cutoff $Y_{in} = 0$. Referring to Fig 3, the load admittance Y_{L2} is the parallel combination between the open-circuited sub and the capacitor B_2,

$$Y_{L2} = jB_2 + jY_{o2}\tan(k_c\, l_2) \tag{11}$$

TABLE 2. Initial dimensions.

Variable	Length (mm)	Variable	Length (mm)
Wr	2	a	11
$g1$	1	$g2$	3.2
l_{C1}	1.27	l_{l1}	1.9
l_{C2}	1.85	l_{l2}	1.95
l_{C3}	1.87	l_{l3}	2
l_{C4}	1.9	l_{l4}	2.05
l_{C5}	1.95	l_{l5}	2.1

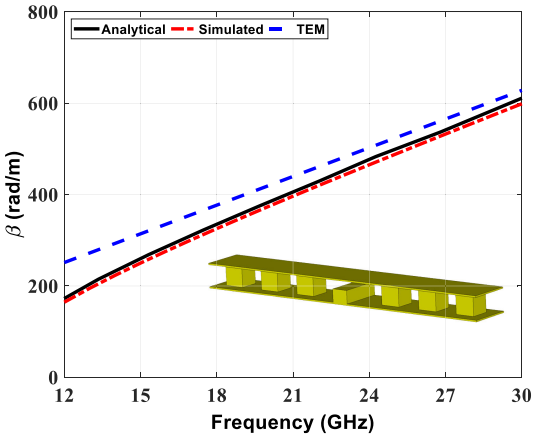

FIGURE 4. Propagation constant verification for row of cells in the X-band.

and the load admittance Y_{L1} is the parallel combination between Y_{L2} and capacitor B

$$Y_{L1} = jB + Y_{o1}\frac{Y_{L2} + jY_{o1}\tan(k_c\, l_1)}{Y_{o1} + jY_{L2}\tan(k_c\, l_1)} \tag{12}$$

and the input admittance will be,

$$Y_{in} = Y_{o3}\frac{Y_{L1} + jY_{o3}\tan(k_c\, l_3)}{Y_{o3} + jY_{L2}\tan(k_c\, l_3)} \tag{13}$$

Therefore, by enforcing the input admittance to be zero $Y_{in} = 0$, we will obtain a transcendental equation as follows,

$$\begin{aligned}&\frac{B}{Y_{o2}} - \frac{B}{Y_{o1}}\Big(\frac{B2}{Y_{o2}} + \tan(k_c\, l_2)\Big)\tan(k_c\, l_1)\\ &\quad + \frac{B_2}{Y_{o2}} + \tan(k_c\, l_2) + \frac{Y_{o1}}{Y_{o2}}\tan(k_c\, l_1)\\ &\quad \frac{Y_{o3}}{Y_{o1}}\tan(k_c\, l_3)\Big[\frac{Y_{o1}}{Y_{o2}} - \Big(\frac{B_2}{Y_{o2}} + \tan(k_c\ \ l_2)\Big)\tan(k_c\, l_1)\Big] = 0\end{aligned} \tag{14}$$

Accordingly, we can solve this transcendental equation and obtain k_c. Finally, the propagation constant β is obtained by the following equation:

$$\beta = \sqrt{k^2 - k_c^2} \tag{15}$$

This equation is verified through several calculations of the propagation constant using CST Microwave studio Eigenmode solver as shown in Figure4. This figure compares the value of the propagation constant obtained from the CST model, the proposed model, and the air propagation constant. The proposed model accurately predicts the value of β for ridge gap waveguide structure. This model offers a good initial point for the phase constant which will be used for designing the LPF, as it will be explained in the following section.

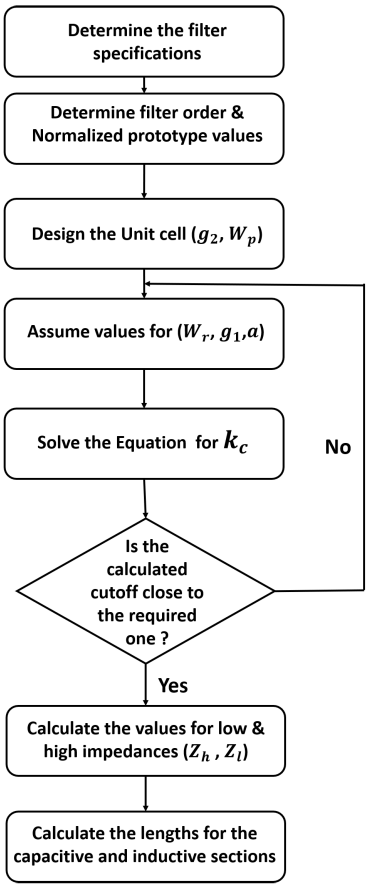

FIGURE 5. Design procedure for RGW LPF.

III. DESIGN PROCEDURE OF THE PROPOSED FILTER

The design procedures for a stepped impedance LPF in RGW can be summarized as shown in the flow chart Figure5. The first step in designing an LPF is determining the filter specification in terms of the pass band, the reject band, the required rejection, and the filter cut-off. Then, the filter order and required ripple level should be determined to get the values for the corresponding capacitors C and inductors L. Afterward, a unit cell is designed to cover the pass and the rejection band of the LPF. The next step is to assume initial values for the ridge width W_r, ridge gap g_1, and distance between the ridge and the bed of nails a_1. Consequently, the equation can be solved and the required virtual cutoff can be obtained. Accordingly, the values for the characteristic impedance of the ridge and the low and high impedances can be found using the parallel plate waveguide approximation [30]. A good initial point for

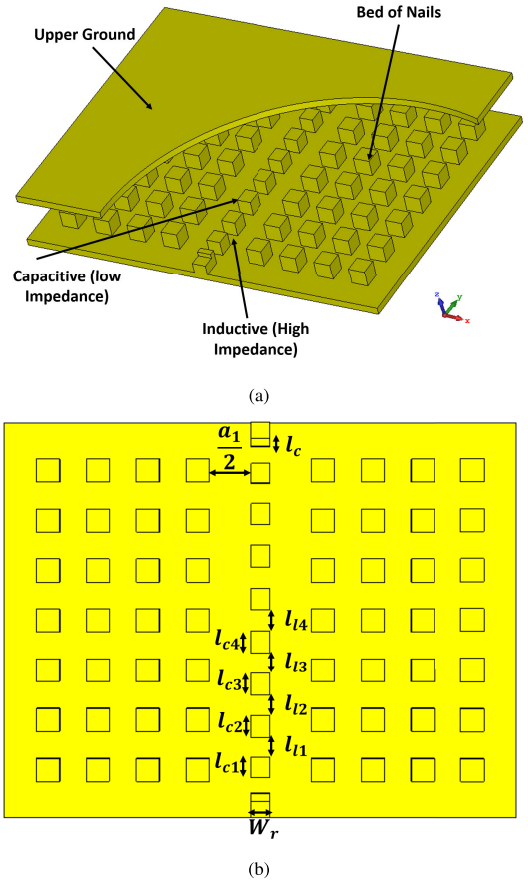

FIGURE 6. RGW filter design, (a) Filter section and (b) Filter variables.

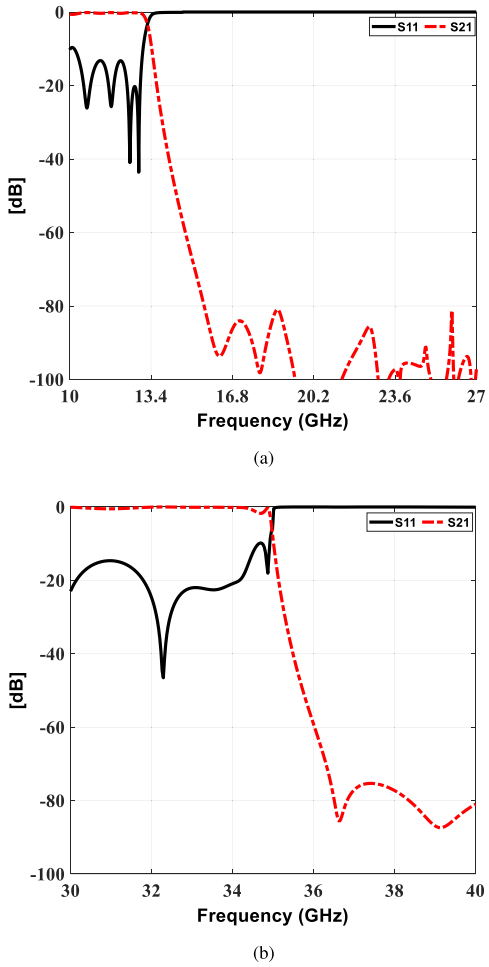

FIGURE 7. Equations verification case for, (a) X-band and (b) Ka-band.

the high and low impedances is three times and half the value of the characteristic impedance respectively. Finally, the lengths of the capacitive and inductive sections can be calculated.

IV. FILTER DESIGN EXAMPLES

In this section, we will verify the above procedure by providing two LPF examples in two different bands (X and Ka) using CST Microwave Studio. The filter shape is shown in Figure6 (a), and the design parameters are the ridge width, lengths for the inductive and capacitive sections, and the distance between the ridge and first unit cell which are indicated in Figure6 (b)

A. FILTER SPECIFICATIONS & EQUATION VALIDATION

The X-band filter is designed to have a passband of [10-13.5] GHz and a rejection of [14.5-27] GHz, while the other filter passband is [30-35.3] GHz and rejection of [36.3-40] GHz. The proposed filter is a low pass filter, as shown in Figure 1 the dispersion diagram indicates the propagation is from 10 GHz to 30 GHz. Accordingly, an additional cut-off frequency is added due to the host guiding structure, where all response curves start at 10 GHz such as in Figure 7 (a) and 9 (d). A 19th-order Chebyshev corrugated filter has been designed to obtain the steep slope between the passband and the rejected band. The design of the LPF uses alternating sections of high and low characteristic impedance lines. This can be realized in the circuit model as alternating capacitors and inductors to represent the required impedances. The values of the normalized prototype (L & C) are obtained based on the filter response and order and they are mentioned in Appendix A. These capacitors and inductors are then realized in ridge gap waveguide technology using posts with different heights as shown in Fig.6.

The lengths for these posts can be calculated using equations (1) and (2), where the virtual propagation constant (β) is determined after solving the transcendental equation. Afterward, the ridge dimensions are calculated by solving the transcendental equation (14), and then a capacitor post is connected to this ridge. The final LPF design is shown in Figure6 and the values for the initial design parameters for the X-band filter are in Table 2. The filters are designed and simulated using CST Microwave Studio, the response of the filters is shown in Figure7. It is clear, that the

TABLE 3. Comparison of the proposed filter and other published filters.

Reference.	f_o (GHz)	IL [dB]	RL [dB]	Rejection [dB]	Dimensions (λ^2)	Technology
[28]	59.7	1.7	9	-60	19.72 × 5.8	GGW
[32]	39.7	1.1	19	-30	3.17 × 0.86	GGW
[33]	30	1.4	15	-90	4.7 × 1.5	MS-RGW
[34]	30.7	2.3	11	-40	3.32 × 1.29	MS-RGW
[35]	14.8	1.35	10	-65	3.29 × 2.26	MS-RGW
[36]	31	2.3	6	-60	0.7 × 0.7	PRGW
[27]	11.6	1	10	-70	14.9 × 4.08	RGW
[37]	35	1	12	-40	1.7 × 1.1	RGW
[38]	21	1.37	14.18	-25	2.93 × 1.93	MS-RGW
[39]	12	1.29	25	-20	0.52 × 0.29	PRGW
[40]	2.5	0.8	18	-	0.15 × 0.08	Microstrip
[41]	11.8	2.24	18	-	0.3 × 1.07	SIW
This Work	13.5	0.7	16.8	-40	2.3 × 2.25	RGW
This Work	35.3	0.7	18	-40	1.8 × 1.5	RGW

cutoff is very close to the intended value $f_c = 13.5$ and $f_c = 35.3$ GHz with an acceptable matching level and rejection. However, the response can be modified further by fine-tuning the parameters as we will discuss in the next subsection.

B. FINAL TUNING & TRANSITION DESIGN

The previous values of the filter are optimized to enhance the matching level of the filter and the optimized values are in Table 4. It is worth mentioning that, the gap for the capacitive cell is not as the gap for the ridge of the RGW. The values for the inductive and capacitive gaps are 3.175 mm and 0.508 mm respectively. Moreover, a transition from a ridge gap waveguide to a single ridge waveguide is designed as shown in Figure8 (a). The values of the LPF with the transition are optimized, so the final response is shown in Figure8 (b) & (c). The optimized values are shown in Table 4, which are very close to the initial values produced from the introduced design procedure. The return loss of the X-band filter is about 20 dB, with an insertion loss of 0.7 dB in the passband, and the rejection band is from 14 GHz to 27 GHz with a 60 dB rejection value. It is worth mentioning that, the higher insertion loss of this filter is due to operation near the dispersion bandwidth of the unit cell. However, the Ka-band filter return loss is roughly 18 dB with 0.7 dB insertion loss and the rejection value is beyond 40 dB from 36 GHz to 40 GHz. The overall dimensions for the X-band and ka-band filters are $(2.3 \times 2.25)\lambda^2$ and $(1.8 \times 1.5)\lambda^2$ respectively.

TABLE 4. Final dimensions.

Variable	Length (mm)	Variable	Length (mm)
Wr	2.5	a	12.23
$g1$	1.27	$g2$	3.2
l_{C1}	0.939	l_{l1}	2.2
l_{C2}	2.359	l_{l2}	2.1844
l_{C3}	2.5	l_{l3}	2.66
l_{C4}	2.54	l_{l4}	2.7
l_{C5}	2.6	l_{l5}	2.8

V. MEASUREMENTS AND VALIDATION

The x-band low pass filter with the two transitions is fabricated using a computer numerical control milling machine with an accuracy of ±0.5 mil, as shown in Fig 9 (a). Moreover, a ridge waveguide calkit is used to measure the response for the filter with the transition as shown in Fig 9 (b). The cutoff of the designed adapters is about 6.36 GHz and can achieve better than -20 dB on the intended band. The measured scattering parameters versus the frequency of the overall structure are illustrated and compared to the simulated curves in Figure9 (c). The transitions are measured back to back and the insertion loss obtained is about 0.6 dB. Therefore, the insertion loss for the proposed filter will be in the range of 0.7 dB. The deviation between the simulated and measured cutoff is due to the fabrication tolerances. It's possible that a human error occurred during the assembly process, which could have arisen from aligning the structure and the ridge. Moreover, placing the upper plate on the filter section may not give the required gap between the LPF center

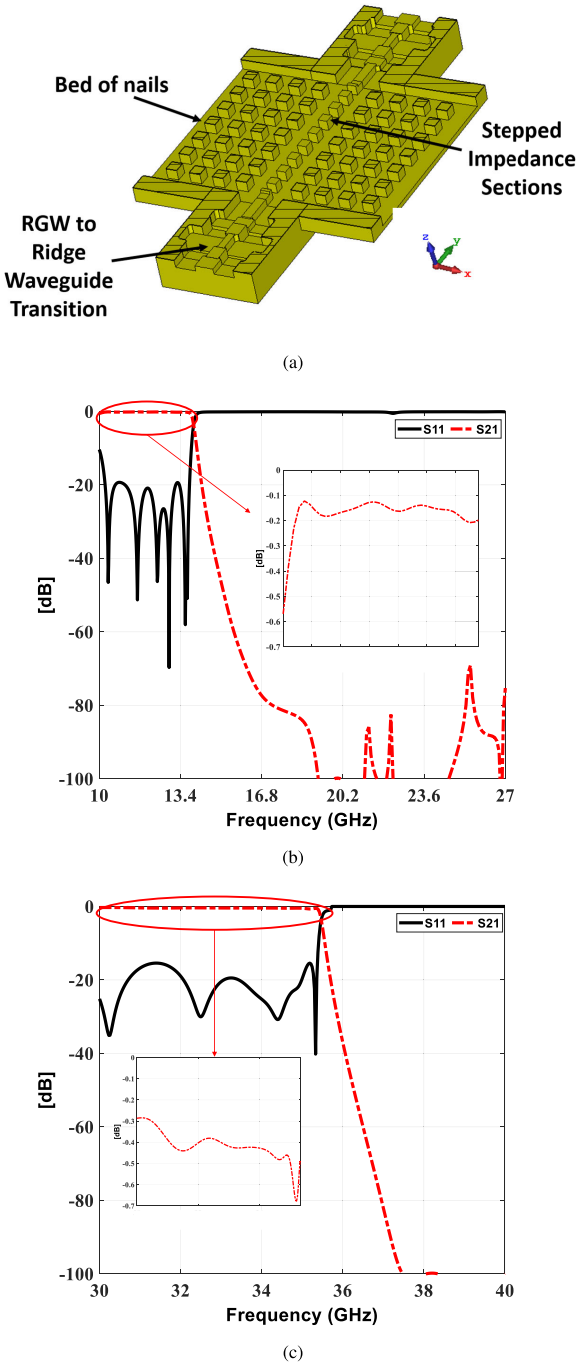

FIGURE 8. LPF with transition, (a) 3D view, (b) Response for X-band, and (c) Ka-band.

section and the upper plate. However, the measured rejection response is still below 60 dB.

VI. PROPOSED FILTER PERFORMANCE EVALUATION

As mentioned previously, this is the first time a low-pass filter is introduced using RGW technology. Thus, Table 3 compared bandpass filters implemented using gap waveguide technologies and two low pass filters implemented using SIW and microstrip technologies. The parameters for these filters

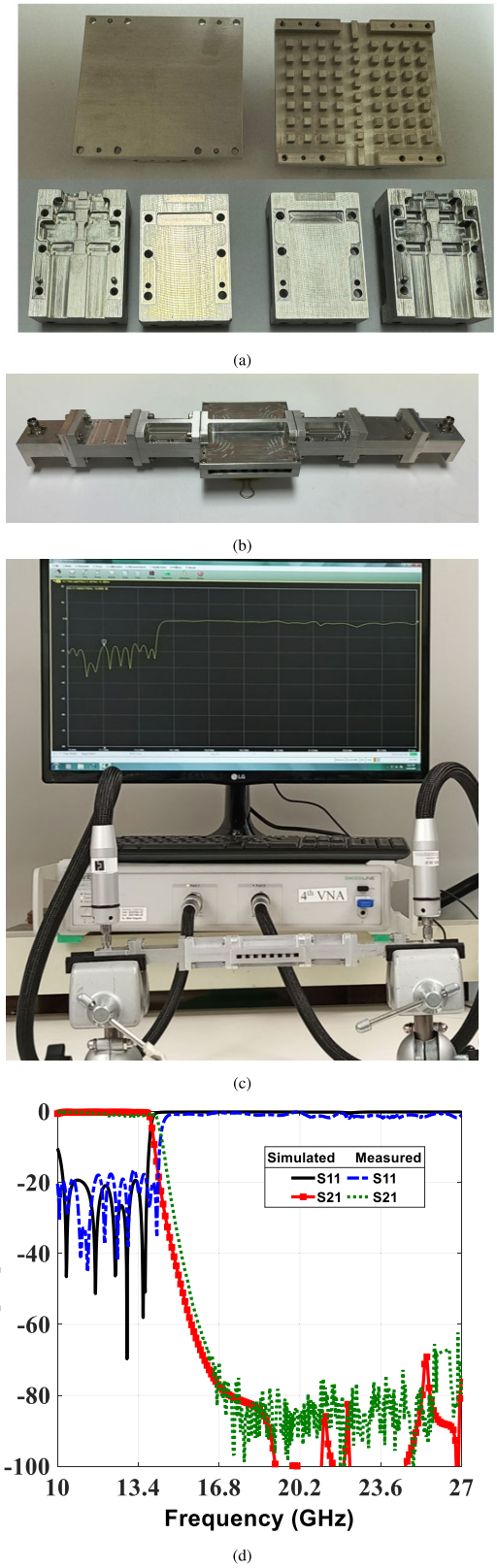

FIGURE 9. Fabricated unit, (a) RGW LPF with transitions, (b) Measuring setup, (c) Measuring setup.

are summarized in Table 3, where f_o denotes filter central frequency, and IL, RL are insertion and the return losses in

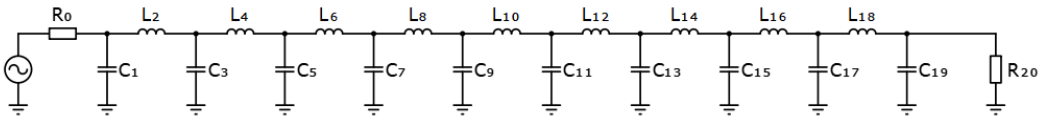

FIGURE 10. Equivalent circuit model.

the passbands, respectively. Table 3 also gives the overall dimensions in wavelengths in the free space λ_o. Moreover, the rejection value for the proposed filters is compared as well. It is worth mentioning that the other filters are bandpass filters, so the rejection for the higher harmonics is not mentioned. The values for the out-band rejection in the table are calculated for 3% after the pass band. In the proposed design, the 60 dB mentioned is the second harmonic rejection value. It is indicated in Table 3 that the size is a clear drawback in most gap waveguide filters [28], [32], [27]. While it could be argued that some published filters are smaller in size [36], it is important to acknowledge that these filters need to be implemented using multiple layers. Furthermore, the PRGW filters exhibit more demanding assembly and increased losses [34], [36]. Some proposed filters outperform them in terms of in-band characteristics, i.e., insertion and return losses [33]. However, the insertion loss and overall dimension of the filter are relatively high.

The proposed filter achieves a deeper matching level with a wider passband and can suppress up to the second harmonic as shown in the X-band filter. It is worth mentioning that some RGW filters achieve good insertion loss values and relatively small size [37]. However, the matching level is not sufficient and the designed filter has a very narrow passband of [34.7-35.3] GHz with rejection up to 36 GHz.

Regarding other technologies, the SIW and microstrip low pass filter show an outstanding performance in terms of return loss and size [40], [41]. However, microstrip-fed networks suffer from high dielectric losses and surface waves at high frequencies [42].

As a result, the suggested structure is a promising option for developing high-quality filters as it satisfies the demands for favorable in-band features and easy production.

VII. CONCLUSION

This paper introduces a novel methodology for designing low-pass filters utilizing RGW technology. It presents a systematic approach and mathematical model for estimating the virtual propagation constant within the ridge gap waveguide. The equations are validated by designing two-stepped impedance low-pass filters using the RGW technology in the X and Ka bands. The ka-band filter return loss and insertion loss are about 18 dB and 0.7 dB respectively. Meanwhile, the X-band filter is constructed and evaluated using a ridge waveguide transition, the fabricated unit achieves a good matching level of approximately 16.8 dB. Moreover, the insertion loss falls within a certain range of 0.7 dB, and the rejection is lower than a certain threshold. In a comparative analysis with previously published filters implemented through various technologies such as RGW, Microstrip, and SIW, the proposed filters excel in terms of return loss and insertion loss, standing out among recent publications.

TABLE 5. L & C values.

Variable	Value (F)	Variable	Value (H)
C_1	0.8736	L_2	1.4773
C_3	1.8914	L_4	1.7716
C_5	2.0251	L_6	1.8294
C_7	2.06	L_8	1.8471
C_9	2.071	L_{10}	1.8515

APPENDIX
STEPPED IMPEDANCE FILTER

The equivalent circuit for the proposed low pass filter consists of nine inductors and ten capacitors, culminating in a 19th-order filter as shown in Figure 10. This configuration is symmetric around the fifth capacitor/inductor C_9 and L_{10}. The specific values for the capacitors and inductors are detailed in Table 5. To implement the effect of the capacitors, posts with a length l_c and height h_c are incorporated into the Ridge Gap Waveguide (RGW). Similarly, the inductors are realized using posts with a length l_l and height h_l. This design approach ensures that the capacitive and inductive elements are effectively realized in the RGW structure, optimizing the filter's performance within the desired frequency range. The values for the lengths of each section are calculated using the following equations

$$\beta l = \frac{L_i Z_o}{Z_h} \tag{16}$$

$$\beta_l = \frac{C_i Z_l}{Z_o} \tag{17}$$

REFERENCES

[1] V. Boria and B. Gimeno, "Waveguide filters for satellites," *IEEE Microw. Mag.*, vol. 8, no. 5, pp. 60–70, Oct. 2007.

[2] G. Maral and M. Bousquet, *Satellite Communication Systems*, 3rd ed. Chichester, U.K.: Wiley, 1998.

[3] C. Kudsia, R. Cameron, and W.-C. Tang, "Innovations in microwave filters and multiplexing networks for communications satellite systems," *IEEE Trans. Microw. Theory Techn.*, vol. 40, no. 6, pp. 1133–1149, Jun. 1992.

[4] R. Coirault, S. J. Feltham, G. Gatti, M. Guglielmi, and D. Perring, "Overview of microwave components activities at the European space agency," *IEEE Trans. Microw. Theory Techn.*, vol. 40, no. 6, pp. 1150–1158, Jun. 1992.

[5] G. L. Matthaei, L. Young, and E. M. T. Jones, *Microwave Filters, Impedance-Matching Networks and Coupling Structures*. New York, NY, USA: McGraw-Hill, 1964.
[6] F. Teberio, I. Arnedo, J. M. Percaz, I. Arregui, T. Lopetegi, and M. A. G. Laso, "Accurate design of corrugated waveguide low-pass filters using exclusively closed-form expressions," in *Proc. 47th Eur. Microw. Conf. (EuMC)*, Oct. 2017, pp. 632–635.
[7] R. J. Cameron, C. M. Kudsia, and R. R. Mansour, *Microwave Filters for Communication Systems: Fundamentals, Design, and Applications*. Hoboken, NJ, USA: Wiley, 2007.
[8] V. E. Boria, P. Soto, and S. Cogollos, "Distributed models for filter synthesis," *IEEE Microw. Mag.*, vol. 12, no. 6, pp. 87–100, Oct. 2011.
[9] M. M. M. Ali, S. I. Shams, and A.-R. Sebak, "Low loss and ultra flat rectangular waveguide harmonic coupler," *IEEE Access*, vol. 6, pp. 38736–38744, 2018.
[10] P.-S. Kildal, A. U. Zaman, E. Rajo-Iglesias, E. Alfonso, and A. Valero-Nogueira, "Design and experimental verification of ridge gap waveguide in bed of nails for parallel-plate mode suppression," *IET Microw., Antennas Propag.*, vol. 5, no. 3, p. 262, 2011.
[11] P.-S. Kildal, "Definition of artificially soft and hard surfaces for electromagnetic waves," *Electron. Lett.*, vol. 24, no. 3, p. 168, 1988.
[12] S. I. Shams and A. A. Kishk, "Ridge gap waveguide to microstrip line transition with perforated substrate," in *Proc. USNC-URSI Radio Sci. Meeting (Joint AP-S Symp.)*, Memphis, TN, USA, Jul. 2014, p. 215.
[13] S. I. Shams and A. A. Kishk, "Wideband coaxial to ridge gap waveguide transition," *IEEE Trans. Microw. Theory Techn.*, vol. 64, no. 12, pp. 4117–4125, Dec. 2016.
[14] S. I. Shams, M. M. Tahseen, and A. A. Kishk, "Wideband relative permittivity characterization of thin low permittivity textile materials based on ridge gap waveguides," *IEEE Trans. Microw. Theory Techn.*, vol. 64, no. 11, pp. 3839–3850, Nov. 2016.
[15] S. I. Shams and A. A. Kishk, "Printed texture with triangle flat pins for bandwidth enhancement of the ridge gap waveguide," *IEEE Trans. Microw. Theory Techn.*, vol. 65, no. 6, pp. 2093–2100, Jun. 2017.
[16] S. I. Shams and A. A. Kishk, "Design of 3-dB hybrid coupler based on RGW technology," *IEEE Trans. Microw. Theory Techn.*, vol. 65, no. 10, pp. 3849–3855, Oct. 2017.
[17] M. A. Abdelaal, S. I. Shams, and A. A. Kishk, "Compact RGW differential phase shifter for millimeter-wave applications," *IEEE Trans. Microw. Theory Tech.*, vol. 66, no. 6, pp. 2767–2774, Jun. 2018.
[18] S. I. Shams, S. M. Sifat, M. Elsaadany, G. Gagnon, and A. A. Kishk, "Systematic design procedure for Y-junction circulator based on ridge gap waveguide technology," *IEEE Trans. Microw. Theory Techn.*, vol. 69, no. 4, pp. 2165–2177, Apr. 2021.
[19] T. Zhang, R. Tang, L. Chen, S. Yang, X. Liu, and J. Yang, "Ultra-wideband full-metal planar array antenna with a combination of ridge gap waveguide and E-plane groove gap waveguide," *IEEE Trans. Antennas Propag.*, vol. 70, no. 9, pp. 8051–8058, Sep. 2022.
[20] T. Li and F. Fan, "Design of Ka-band 2×2 circular polarization slot antenna array fed by ridge gap waveguide," in *Proc. 6th Asia–Pacific Conf. Antennas Propag. (APCAP)*, Oct. 2017, pp. 1–3.
[21] Z. Zang, A. U. Zaman, and J. Yang, "Design of dual circularly polarized inclined slot pair based on stepped-height ridge gap waveguide with series excitation," in *Proc. 16th Eur. Conf. Antennas Propag. (EuCAP)*, Mar. 2022, pp. 1–5.
[22] D. Sun and J. Xu, "A novel iris waveguide bandpass filter using air gapped waveguide technology," *IEEE Microw. Wireless Compon. Lett.*, vol. 26, no. 7, pp. 475–477, Jul. 2016.
[23] T. Xiu, Y. Yao, H. Jiang, X. Cheng, C. Wang, B. Wang, J. Yu, and X. Chen, "Design of a compact and low-loss E-band filter based on multilayer groove gap waveguide," *IEEE Microw. Wireless Compon. Lett.*, vol. 31, no. 11, pp. 1211–1214, Nov. 2021.
[24] A. U. Zaman, P.-S. Kildal, and A. A. Kishk, "Narrow-band microwave filter using high-Q groove gap waveguide resonators with manufacturing flexibility and no sidewalls," *IEEE Trans. Compon., Packag., Manuf. Technol.*, vol. 2, no. 11, pp. 1882–1889, Nov. 2012.
[25] J.-Y. Deng, M.-J. Li, D. Sun, L.-X. Guo, and X.-H. Ma, "Compact dual-band inverted-microstrip ridge gap waveguide bandpass filter," *IEEE Trans. Microw. Theory Techn.*, vol. 68, no. 7, pp. 2625–2632, Jul. 2020.
[26] M. Sharifi Sorkherizi and A. A. Kishk, "Self-packaged, low-loss, planar bandpass filters for millimeter-wave application based on printed gap waveguide technology," *IEEE Trans. Compon., Packag., Manuf. Technol.*, vol. 7, no. 9, pp. 1419–1431, Sep. 2017.
[27] M. S. Sorkherizi, A. Khaleghi, and P.-S. Kildal, "Direct-coupled cavity filter in ridge gap waveguide," *IEEE Trans. Compon., Packag., Manuf. Technol.*, vol. 4, no. 3, pp. 490–495, Mar. 2014.
[28] M. Rezaee, A. U. Zaman, and P.-S. Kildal, "A groove gap waveguide iris filter for V-band application," in *Proc. 23rd Iranian Conf. Electr. Eng.*, May 2015, pp. 462–465.
[29] D. M. Pozar, *Microwave Engineering*, 4th ed. Hoboken, NJ, USA: Wiley, 2011.
[30] E. Alfonso, P.-S. Kildal, A. Valero-Nogueira, and M. Baquero, "Study of the characteristic impedance of a ridge gap waveguide," in *Proc. IEEE Antennas Propag. Soc. Int. Symp.*, Jun. 2009, pp. 1–4.
[31] J. Helszajn, *Ridge Waveguides and Passive Microwave Components*. Edison, NJ, USA: IET, Jun. 2000.
[32] A. del Olmo-Olmeda, M. Baquero-Escudero, V. E. Boria-Esbert, A. Valero-Nogueira, and A. J. Berenguer-Verdú, "A novel band-pass filter topology for millimeter-wave applications based on the groove gap waveguide," in *IEEE MTT-S Int. Microw. Symp. Dig.*, Jun. 2013, pp. 1–4.
[33] F. Fan, Z. Yan, J. Wang, and X. Song, "KA band-pass filter based on the microstrip-groove gap waveguide technology," in *Proc. IET Int. Radar Conf.*, Oct. 2015, pp. 1–4.
[34] M. S. Sorkherizi and A. A. Kishk, "Lowloss planar bandpass filters for millimeter-wave application," in *IEEE MTT-S Int. Microw. Symp. Dig.*, May 2015, pp. 1–4.
[35] S. Birgermajer, N. Jankovic, V. Radonic, V. Crnojevic-Bengin, and M. Bozzi, "Microstrip-ridge gap waveguide filter based on cavity resonators with mushroom inclusions," *IEEE Trans. Microw. Theory Techn.*, vol. 66, no. 1, pp. 136–146, Jan. 2018.
[36] M. S. Sorkherizi and A. A. Kishk, "Fully printed gap waveguide with facilitated design properties," *IEEE Microw. Wireless Compon. Lett.*, vol. 26, no. 9, pp. 657–659, Sep. 2016.
[37] B. Ahmadi and A. Banai, "Direct coupled resonator filters realized by gap waveguide technology," *IEEE Trans. Microw. Theory Techn.*, vol. 63, no. 10, pp. 3445–3452, Oct. 2015.
[38] Z.-H. Shi, F. Wei, L. Yang, and R. Gómez-García, "High-selectivity inverted microstrip gap waveguide bandpass filter using hybrid cavity and stub-loaded ring resonant modes," *IEEE Trans. Circuits Syst. II, Exp. Briefs*, vol. 71, no. 1, pp. 146–150, Jan. 2024.
[39] J.-Y. Deng, D.-D. Yuan, J.-Y. Yin, D. Sun, L.-X. Guo, X.-H. Ma, and Y. Hao, "Ultracompact bandpass filter based on slow wave substrate integrated groove gap waveguide," *IEEE Trans. Microw. Theory Techn.*, vol. 70, no. 2, pp. 1211–1220, Feb. 2022.
[40] S. Luo, L. Zhu, and S. Sun, "Stopband-expanded low-pass filters using microstrip coupled-line hairpin units," *IEEE Microw. Wireless Compon. Lett.*, vol. 18, no. 8, pp. 506–508, Aug. 2008.
[41] T. Yun, H. Nam, J. Kim, B. Lee, J. Choi, K. Kim, T. Ha, and J. Lee, "Harmonics suppressed substrate-integrated waveguide filter with integration of low-pass filter," *Microw. Opt. Technol. Lett.*, vol. 50, no. 2, pp. 447–450, Feb. 2008.
[42] A. Borji, D. Busuioc, and S. Safavi-Naeini, "Efficient, low-cost integrated waveguide-fed planar antenna array for Ku-band applications," *IEEE Antennas Wireless Propag. Lett.*, vol. 8, pp. 336–339, 2009.

MAHMOUD GADELRAB (Student Member, IEEE) received the B.Sc. degree in communications engineering from German University in Cairo (GUC), in 2021. He is currently pursuing the master's degree with Concordia University. His research interests include ferrite-based structures, ridge gap waveguide technologies, and satellite-feeding structures. He received the GUC Top Ranking Students Scholarship, in 2016, and maintained this award, until 2021. He also received the Concordia Supervisor's Research Grant for the Master of Applied Science.

SHOUKRY I. SHAMS (Senior Member, IEEE) received the B.Sc. (Hons.) and M.Sc. degrees in electronics and communications engineering from Cairo University, Cairo, Egypt, in 2004 and 2009, respectively, and the Ph.D. degree in electrical and computer engineering from Concordia University, Montreal, QC, Canada, in 2016. From 2005 to 2006, he was a Teaching and Research Assistant with the Department of Electronics and Communications Engineering, Cairo University. From 2006 to 2012, he was a Teaching and Research Assistant with the Institute of Engineering and Technology (IET) Department, German University in Cairo. From 2012 to 2016, he was a Teaching and Research Assistant with Concordia University. His research interests include microwave reciprocal/nonreciprocal design and analysis, high-power microwave subsystems, antenna design, and material measurement. He received the Faculty Certificate of Honor, in 1999, and the Distinction with Honor, in 2004, from Cairo University. He was a recipient of the Concordia University Recruitment Award, in 2012, and the Concordia University Accelerator Award, in 2016. He was the German University in Cairo (GUC)-IEEE Student Branch Chair, from 2010 to 2012.

MAHMOUD ELSAADANY (Senior Member, IEEE) received the B.Sc. (Hons.) and M.Sc. degrees in electrical engineering from Cairo University, Giza, Egypt, in 2006 and 2010, respectively, and the Ph.D. degree in electrical and computer engineering from Concordia University, Montreal, QC, Canada, in 2018. He was a Researcher with Qatar University, Doha, Qatar, from 2008 to 2010. He is currently an Assistant Professor with the ECE Department, Concordia University, and a Research Professor with École de Technologie Supérieure (ETS), Université du Québec, Montreal. His current research interests include digital signal processing, optimization of microwave components, machine-type communication, and algorithm design for 5G cellular networks.

ABDELRAZIK SEBAK (Life Fellow, IEEE) received the B.Sc. degree (Hons.) in electrical engineering from Cairo University, Cairo, Egypt, in 1976, the B.Sc. degree in applied mathematics from Ain Shams University, Cairo, in 1978, and the M.Eng. and Ph.D. degrees in electrical engineering from the University of Manitoba, Winnipeg, MB, Canada, in 1982 and 1984, respectively. From 1984 to 1986, he was with Canadian Marconi Company, where he was involved in the design of microstrip phased array antennas. From 1987 to 2002, he was a Professor with the Department of Electronics and Communication Engineering, University of Manitoba. He is currently a Professor with the Department of Electrical and Computer Engineering, Concordia University, Montreal, QC, Canada. His research interests include phased-array antennas, millimeter-wave antennas and imaging, computational electromagnetics, and the interaction of EM waves with engineered materials and bioelectromagnetics. He is a member of Canadian National Committee of the International Union of Radio Science Commission B. He was a recipient of the 2000 and 1992 University of Manitoba Merit Award for Outstanding Teaching and Research, the 1994 Rh Award for Outstanding Contributions to Scholarship and Research, and the 1996 Faculty of Engineering Superior. He served as the Chair for the IEEE Canada Awards and Recognition Committee, from 2002 to 2004, and the Technical Program Chair for the 2002 IEEE CCECE Conference and the 2006 URSIANTEM Symposium. He was the Technical Program Co-Chair of the 2015 IEEE ICUWB Conference.